Hopf Bifurcation at Infinity in 3D symmetric piecewise linear systems. Application to a Bonhoeffer-Van der Pol oscillator

E. Freire[1], E. Ponce[2], J. Ros[3], E. Vela[4]

Departamento de Matemática Aplicada II and Instituto de Matemáticas (IMUS), Escuela Técnica Superior de Ingeniería, Avda. de los Descubrimientos, 41092 Sevilla, Spain

A. Amador[5]

Facultad de Ingeniería y Ciencias, Departamento de Ciencias Naturales y Matemáticas, Pontificia Universidad Javeriana - Cali, Santiago de Cali, Colombia

Abstract

In this work, a Hopf bifurcation at infinity in three-dimensional symmetric continuous piecewise linear systems with three zones is analized. By adapting the so-called closing equations method, which constitutes a suitable technique to detect limit cycles bifurcation in piecewise linear systems, we give for the first time a complete characterization of the existence and stability of the limit cycle of large amplitude that bifurcates from the point at infinity. Analytical expressions for the period and amplitude of the bifurcating limit cycles are obtained. As an application of these results, we study the appearance of a large amplitude limit cycle in a Bonhoeffer-Van der Pol oscillator.

[1]efrem@us.es
[2]eponcem@us.es
[3]javieros@us.es
[4]elivela@us.es
[5]afamador@javerianacali.edu.co

Keywords: Piecewise linear systems, bifurcations at infinity, Hopf bifurcation, Bonhoeffer-Van der Pol oscillator

1. Introduction

For sufficiently smooth differential systems the Poincaré-Andronov-Hopf bifurcation theorem provides a general explanation for the birth of a small amplitude limit cycle surrounding a certain equilibrium point when two eigenvalues of the linearization at the point cross the imaginary axis, see for instance [1, 2, 3, 4]. There are situations however, both for smooth and non-smooth systems, where limit cycles appear or disappear with great amplitude, coming from or going to infinity; then it is said that a Hopf bifurcation at infinity takes place, see for instance [5, 6, 7, 8, 9, 10, 11, 12].

To the best of our knowledge, one of the first publications about the Hopf bifurcation at infinity appeared in [13], by adapting ideas from the Hopf bifurcation at the origin taken from [14]. Another general study is done in [15], where, by means of techniques of parameter functionalization and methods of monotone concave and convex operators, authors show the existence, uniqueness, and stability of large-amplitude periodic cycles arising in Hopf bifurcations at infinity for autonomous control systems with bounded nonlinear feedback. Here, we will consider the general case of 3D symmetric continuous piecewise linear systems with three zones, looking for an alternative approach to the quoted works that gives more quantitative information on the bifurcating limit cycle.

Piecewise linear systems have a notable, rather long pedigree. For instance, in the seminal book of Andronov [16], there appears a plenty of

mechanical, electrical and control applications whose nonlinearities are adequately modeled as piecewise linear functions. They also have played a remarkable role in the advance of nonlinear dynamics; as an outstanding example, we could remind how the work by Norman Levinson [17] on the forced VanderPol equation with a piecewise constant nonlinearity was crucial in the discovering of the horseshoe paradigm by Steve Smale [18]. In particular, the class of continuous piecewise linear (CPWL, for short) systems has been used in diverse areas to accurately model many physical phenomena, sometimes involving abrupt events or fast transitions. For three-dimensional piecewise linear systems with two or three zones, different phenomena as bistability, hysteresis, instantaneous transitions of a stable equilibrium to chaotic attractor, as well as the existence of limit cycles of great amplitude have been reported, see for instance [19, 20, 21, 22, 23].

A suitable technique to detect limit cycles bifurcation in piecewise linear systems is the so-called closing equations method. This method involves the integration of the system in each linear zone and the subsequent matching of solutions, and allows to obtain expressions for the period and amplitude of the bifurcating limit cycle, see for instance [24, 25, 26, 27, 28]. The method needs to be adapted to deal with limit cycles of great amplitude, as firstly proposed in [29]. Here, we show in detail how such method can be suited to the study of periodic orbits of large amplitude in three-dimensional symmetric continuous piecewise linear systems with three zones. We obtain general results for quantitative estimates of the period and the amplitude, also determining the stability of the bifurcating limit cycle. As a direct application of the previous results, we characterize one unreported bifurcation of limit cycles

of great amplitude in a piecewise linear Bonhoeffer-Van der Pol oscillator [30, 31, 32].

The paper is organized as follows. After a detailed setting of the problem and some auxiliary results, the main contributions of the work are Theorem 5 and Corollary 6, both presented in Section 2. The theoretical results are applied to a Bonhoeffer-Van der Pol electronic oscillator in Section 3. In Section 4, we show how our work improves a previous related result [15]. The proof of Theorem 5 is delayed to Section 5 for ease of reading. For the same reason, other auxiliary material is relegated to Appendix A, which appears after a section devoted to some concluding remarks.

2. Introduction to modified closing equations and main results

We start by considering a piecewise linear system in $\mathbb{R}^3$ defined by

$$\dot{\mathbf{x}} = \begin{cases} \mathbf{A}_E\mathbf{x} + \mathbf{b}, & \text{if} \quad \mathbf{e}_1^\top\mathbf{x} < -1, \\ \mathbf{A}_C\mathbf{x}, & \text{if} \quad |\mathbf{e}_1^\top\mathbf{x}| \leq 1, \\ \mathbf{A}_E\mathbf{x} - \mathbf{b}, & \text{if} \quad \mathbf{e}_1^\top\mathbf{x} > 1, \end{cases} \tag{1}$$

where $\mathbf{x} = (x, y, z)^\top$, $\mathbf{e}_1$ is the first canonical vector, the vector $\mathbf{b} \in \mathbb{R}^3$ is constant and the matrices $\mathbf{A}_{\{C,E\}}$ are the 3×3 constant real matrices that rule the dynamics in the central (C) and external (E) zones, which share the last two columns. Therefore, system (1) is a symmetric continuous piecewise linear system with three linearity zones separated by two parallel planes defined by

$$\Sigma_1 = \{\mathbf{x} \in \mathbb{R}^3 : \mathbf{e}_1^\top\mathbf{x} = 1\}, \quad \Sigma_{-1} = \{\mathbf{x} \in \mathbb{R}^3 : \mathbf{e}_1^\top\mathbf{x} = -1\}. \tag{2}$$

These sets define three regions of $\mathbb{R}^3$ where $\mathbf{e}_1^\top \mathbf{x} < -1$, $|\mathbf{e}_1^\top \mathbf{x}| \leq 1$ and $\mathbf{e}_1^\top \mathbf{x} > 1$ and will be denoted by L (left), C (central) and R (right) zones. Due to the symmetry of the vector field, we use the symbol E to denote both the left and the right external zones.

After a linear change of variables (see Proposition 16 of [33]), system (1) can be rewritten into the so-called generalized Lienard's form given by

$$\dot{\mathbf{x}} = \begin{pmatrix} t_E & -1 & 0 \\ m_E & 0 & -1 \\ d_E & 0 & 0 \end{pmatrix} \mathbf{x} + \begin{pmatrix} t_C - t_E \\ m_C - m_E \\ d_C - d_E \end{pmatrix} \text{sat}\left(\mathbf{e}_1^\top \mathbf{x}\right), \tag{3}$$

where $t_{\{C,E\}}$, $m_{\{C,E\}}$ and $d_{\{C,E\}}$ are the linear invariants (trace, sum of principal minors and determinant) of the matrices $\mathbf{A}_C$ and $\mathbf{A}_E$, respectively, and where $\text{sat}\,(x)$ is the normalized saturation function

$$\text{sat}\,(x) = \begin{cases} x & \text{if} \quad |x| \leq 1, \\ \text{sgn}(x) & \text{if} \quad |x| > 1. \end{cases}$$

We remark that for $|x| \leq 1$ system (3) becomes $\dot{x} = \mathbf{A}_C x$ with

$$\mathbf{A}_C = \begin{pmatrix} t_C & -1 & 0 \\ m_C & 0 & -1 \\ d_C & 0 & 0 \end{pmatrix}, \tag{4}$$

so that the solutions in the central zone can be written as

$$\mathbf{x}(\tau) = e^{\mathbf{A}_C \tau} \mathbf{x}(0), \tag{5}$$

where the vector $\mathbf{x}(0)$ denotes the selected initial conditions.

The case $d_E = \det(\mathbf{A}_E) = 0$ corresponds to a degenerated situation, corresponding to a pitchfork bifurcation at infinity, and in what follows we

assume $d_E \neq 0$. Under this generic condition, apart from the origin, system (3) always has the two additional equilibrium points $\overline{\mathbf{x}}_R$ and $\overline{\mathbf{x}}_L$ (to be virtual or real), where

$$\overline{\mathbf{x}}_R = -\mathbf{A}_E^{-1} b = \frac{1}{d_E} \begin{pmatrix} d_E - d_C \\ t_C d_E - t_E d_C \\ m_C d_E - m_E d_C \end{pmatrix}, \quad \overline{\mathbf{x}}_L = -\overline{\mathbf{x}}_R, \tag{6}$$

so that the solutions $\mathbf{x}(\tau)$ in the external zones can be written as

$$\mathbf{x}(\tau) = \overline{\mathbf{x}}_{\{L,R\}} + e^{\mathbf{A}_E \tau}(\mathbf{x}(0) - \overline{\mathbf{x}}_{\{L,R\}}). \tag{7}$$

Note that if $d_C d_E < 0$ then there exist three real equilibria, as it is easily concluded checking the first component of (6).

Assume the existence of a symmetric limit cycle in system (3) living in the regions L, C and R and with four transversal intersection points with the planes Σ_1 and Σ_{-1}, respectively $\mathbf{x}_0$, $\mathbf{x}_3$ and $\mathbf{x}_1$, $\mathbf{x}_2$, see Figure 1. Due to the symmetry, it will be fulfilled $\mathbf{x}_2 = -\mathbf{x}_0 \in \Sigma_{-1}$ and $\mathbf{x}_3 = -\mathbf{x}_1 \in \Sigma_1$.

Using solution (5) in zone C with $\mathbf{x}(0) = \mathbf{x}_0$, where

$$\mathbf{x}_0 = \begin{pmatrix} 1 \\ y_0 \\ z_0 \end{pmatrix} \in \Sigma_1, \tag{8}$$

with $y_0 > t_C$ (so that $\dot{x} < 0$ at $\mathbf{x}_0$) and assuming a flight time $\tau = \tau_C$, to arrive at $\mathbf{x}_1$, we will have

$$\mathbf{x}_1 = \begin{pmatrix} -1 \\ y_1 \\ z_1 \end{pmatrix} \in \Sigma_{-1},$$

and we obtain the condition

$$\begin{pmatrix} -1 \\ y_1 \\ z_1 \end{pmatrix} = e^{\mathbf{A}_C \tau_C} \begin{pmatrix} 1 \\ y_0 \\ z_0 \end{pmatrix}.$$

Using solution (7) in zone L with $\mathbf{x}(0) = \mathbf{x}_1$, where

$$\mathbf{x}_1 = \begin{pmatrix} -1 \\ y_1 \\ z_1 \end{pmatrix} \in \Sigma_{-1}, \tag{9}$$

with $y_1 > -t_C$ and assuming a flight time $\tau = \tau_E$, to arrive at the point $\mathbf{x}_2$, so that

$$\mathbf{x}(\tau_E) = \mathbf{x}_2 = -\mathbf{x}_0 = -\begin{pmatrix} 1 \\ y_0 \\ z_0 \end{pmatrix} \in \Sigma_{-1},$$

we obtain a new condition, that is,

$$-\mathbf{x}_0 - \overline{\mathbf{x}}_L = e^{\mathbf{A}_E \tau_E}(\mathbf{x}_1 - \overline{\mathbf{x}}_L).$$

Therefore, it is possible to identify symmetric limit cycles of system (3) with the solutions of the equations

$$\begin{aligned} e^{\mathbf{A}_C \tau_C}\mathbf{x}_0 - \mathbf{x}_1 &= \mathbf{0}, \\ e^{\mathbf{A}_E \tau_E}(\mathbf{x}_1 - \overline{\mathbf{x}}_L) + \mathbf{x}_0 + \overline{\mathbf{x}}_L &= \mathbf{0}, \end{aligned} \tag{10}$$

where τ_C and τ_E are the times spent by the semi-orbit in each zone, and $\mathbf{x}_0$, $\mathbf{x}_1$ and $\overline{\mathbf{x}}_L$ are defined in (8), (9) and (6) respectively. Equations (10) will be referred to as the closing equations. The use of these equations goes back to Andronov and coworkers [16] and have been previously used for the analysis of limit cycle bifurcations, see for instance [25, 26, 34, 35, 36].

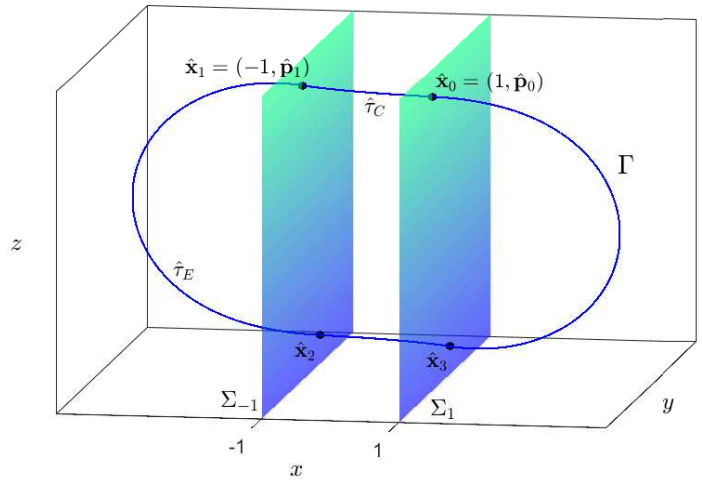

Figure 1: A symmetric limit cycle, using the three linearity zones of system (3), and some distinguished points.

The above closing equations allow also to analyze the stability of the closed orbits by studying the behavior of an adequate return map near the periodic orbit. If $\hat{\mathbf{x}}_0$, $\hat{\mathbf{x}}_1$ are the intersection points of given symmetric periodic orbit, due to the symmetry of system (1), we only need to consider orbits that start at Σ_1 near $\hat{\mathbf{x}}_0 \in \Sigma_1$, and look for their crossing points at Σ_{-1} near $\hat{\mathbf{x}}_1 \in \Sigma_{-1}$ and next, look at the return points at Σ_{-1} near $-\hat{\mathbf{x}}_0 \in \Sigma_{-1}$ (see Figure 1). For such near points, we denote by $\mathbf{p}_0$, $\mathbf{p}_1 \in \mathbb{R}^2$, the coordinates of $\mathbf{x}_0$ and $\mathbf{x}_1$ restricted to their respective sections, so that $\mathbf{x}_0 = (1, \mathbf{p}_0)^\top \in \Sigma_1$ and $\mathbf{x}_1 = (-1, \mathbf{p}_1)^\top \in \Sigma_{-1}$. From the transition maps associated to the flow, locally defined at the points $\hat{\mathbf{x}}_0$ and $\hat{\mathbf{x}}_1$, it is possible to define in adequate neighborhoods at the sections the functions providing the corresponding restricted coordinates and flight times. Let us denote by

π_C, π_E such functions, satisfying $\pi_C(\hat{\mathbf{p}}_0) = \hat{\mathbf{p}}_1$, $\pi_E(\hat{\mathbf{p}}_1) = -\hat{\mathbf{p}}_0$, and let π_{EC} be its composition $\pi_{EC} = \pi_E \circ \pi_C$. We will denote by $\tau_C(\mathbf{p}_0)$ and $\tau_E(\mathbf{p}_1)$ the times spent by near orbits in passing from generic points $\mathbf{x}_0$ to $\mathbf{x}_1$, and from $\mathbf{x}_1$ to $\mathbf{x}_2$, respectively, in the adequate sections, and we will use $D_{\mathbf{p}}(\cdot)$ to indicate their derivatives with respect to the restricted coordinates. The following results will be useful to determine the stability of any symmetric limit cycle, sense they allow to complete in an easy way its characteristic multipliers.

Proposition 1. *Consider a transversal symmetric periodic orbit* Γ *of system* (1) *that uses the three zones of linearity and intersects transversally* Σ_1 *at the point* $\hat{\mathbf{x}}_0 = (1, \hat{\mathbf{p}}_0)^\top$ *and* $\hat{\mathbf{x}}_3$*, and* Σ_{-1} *at* $\hat{\mathbf{x}}_1 = (-1, \hat{\mathbf{p}}_1)^\top$ *and* $\hat{\mathbf{x}}_2$*, where* $\hat{\mathbf{x}}_3 = -\hat{\mathbf{x}}_1$*,* $\hat{\mathbf{x}}_2 = -\hat{\mathbf{x}}_0$*, with times* $\hat{\tau}_C = \tau_C(\hat{\mathbf{p}}_0)$ *and* $\hat{\tau}_E = \tau_E(\hat{\mathbf{p}}_1)$ *in zones* C *and* L *respectively, see Figure 1. Then, the product of the next two matrices*

$$\begin{pmatrix} 1 & D_{\mathbf{p}}\tau_E(\hat{\mathbf{p}}_1) \\ \mathbf{0} & D_{\mathbf{p}}\pi_E(\hat{\mathbf{p}}_1) \end{pmatrix} \begin{pmatrix} -1 & D_{\mathbf{p}}\tau_C(\hat{\mathbf{p}}_0) \\ \mathbf{0} & D_{\mathbf{p}}\pi_C(\hat{\mathbf{p}}_0) \end{pmatrix} = \begin{pmatrix} -1 & D_{\mathbf{p}}\tau_C(\hat{\mathbf{p}}_0) + D_{\mathbf{p}}\tau_E(\hat{\mathbf{p}}_1) D_{\mathbf{p}}\pi_C(\hat{\mathbf{p}}_0) \\ \mathbf{0} & D_{\mathbf{p}}\pi_{EC}(\hat{\mathbf{p}}_0) \end{pmatrix}$$

is similar to the matrix

$$\mathbf{M} = e^{\mathbf{A}_E \hat{\tau}_E} e^{\mathbf{A}_C \hat{\tau}_C}. \tag{11}$$

Proposition 1 is shown in Appendix A. Consequently, the product in (11) has always an eigenvalue equal to -1. More precisely, we can state the following corollary.

Corollary 2. *Let* Γ *be a symmetric periodic orbit of system* (1)*, under hypotheses of Proposition 1. Then, an eigenvalue of*

$$e^{\mathbf{A}_E \hat{\tau}_E} e^{\mathbf{A}_C \hat{\tau}_C}$$

is -1 *and the squares of the remaining two eigenvalues are the characteristic multipliers of the periodic orbit* Γ.

To simplify the subsequent analysis, it is useful to take into account the following result.

Remark 3. *To lower the dimension of closing equations* (10)*, it is useful to rewrite the equations in the equivalent form*

$$\begin{aligned} e^{\mathbf{A}_C\tau_C}\mathbf{x}_0 - \mathbf{x}_1 &= \mathbf{0}, \\ \mathbf{x}_1 - \overline{\mathbf{x}}_L + e^{-\mathbf{A}_E\tau_E}(\mathbf{x}_0 + \overline{\mathbf{x}}_L) &= \mathbf{0}, \end{aligned} \tag{12}$$

so that we can eliminate the coordinates y_1*,* z_1 *in the vector* $\mathbf{x}_1$ *by considering only the equation*

$$e^{\mathbf{A}_C\tau_C}\mathbf{x}_0 - \overline{\mathbf{x}}_L + e^{-\mathbf{A}_E\tau_E}(\mathbf{x}_0 + \overline{\mathbf{x}}_L) = \mathbf{0}, \tag{13}$$

along with the corresponding condition to the first coordinate of (10)*, namely*

$$\mathbf{e}_1^\top e^{\mathbf{A}_C\tau_C}\mathbf{x}_0 + 1 = \mathbf{0}, \tag{14}$$

what gives us a system with only four equations.

In order to deal with orbits of large amplitude for system (3), a new set of equations is introduced as follows. A reference coordinate for the intersection of the orbit with the plane Σ_1 is chosen, say y_0 (it is generically assumed for a large amplitude periodic orbit that y_0 is positive and sufficiently big, satisfying $y_0 > t_C$), and we define a new change of variables by using the normalized coordinates

$$r_0 = \frac{1}{y_0}, \quad v_0 = \frac{z_0}{y_0}. \tag{15}$$

Consequently, after multiplying all the equations of (13) and (14) by r_0, it becomes

$$\begin{aligned} \mathbf{e}_1^\top e^{\mathbf{A}_C\tau_C}\left(r_0,1,v_0\right)^\top + r_0 = 0,\\ e^{\mathbf{A}_C\tau_C}\left(r_0,1,v_0\right)^\top - r_0\overline{\mathbf{x}}_L + e^{-\mathbf{A}_E\tau_E}\left[\left(r_0,1,v_0\right)^\top + r_0\overline{\mathbf{x}}_L\right] = \mathbf{0}. \end{aligned} \tag{16}$$

In fact, if we have a branch of solutions of equations (16) and by moving parameters we make r_0 to tend to 0, then the corresponding periodic orbit will approach a certain periodic orbit at infinity. This new set of closing equations will be analyzed for small $r_0 > 0$, corresponding to large amplitude limit cycles with a very large value for $y_0 > 0$. Therefore, these equations are useful to detect the bifurcation of a limit cycle from the periodic orbit at infinity of system (3) that corresponds to the solution of (16) with $\tau_C = 0$, $\tau_E > 0$, $r_0 = 0$, $v_0 = t_E$ and $m_E t_E - d_E = 0$ with $m_E > 0$; more precisely, we have the following result.

Lemma 4. *The unique solution of equations* (16) *with* $\tau_C = 0$, $d_E \neq 0$ *and* $\tau_E > 0$ *is* $r_0 = 0$, $v_0 = t_E$ *and* $\tau_E = \pi/\sqrt{m_E}$, *with* $m_E t_E - d_E = 0$ *and* $m_E > 0$.

Proof. For $\tau_C = 0$, the first equation of (16) is equivalent to $2r_0 = 0$ what implies $r_0 = 0$. Substituting $\tau_C = 0$ and $r_0 = 0$ in the other equations of (16) we obtain the equivalent condition

$$e^{\mathbf{A}_E\tau_E}\begin{pmatrix} 0\\ 1\\ v_0 \end{pmatrix} + \begin{pmatrix} 0\\ 1\\ v_0 \end{pmatrix} = \mathbf{0}, \tag{17}$$

what tells us that the matrix $\exp\left(\mathbf{A}_E\tau_E\right)$ has an eigenvector of the form $(0,1,v_0)^\top$ corresponding to the eigenvalue -1. If μ_E is the eigenvalue of $\mathbf{A}_E$

corresponding to the eigenvalue -1 of the matrix exponential, then we will have $e^{\mu_E \tau_E} = -1$, what implies $\mu_E \tau_E = \pi i$, so that μ_E is pure imaginary. Therefore, for the values $\tau_C = 0$ and $r_0 = 0$, the matrix $\mathbf{A}_E$ has a pair of imaginary eigenvalues that we will denote by $\pm\omega i$, with $\omega > 0$, and so $\omega \tau_E = \pi$. Obviously, the third eigenvalue must be real, say λ, and the following equalities hold

$$t_E = \lambda, \quad m_E = \omega^2, \quad d_E = \lambda\omega^2. \tag{18}$$

The above equalities are equivalent to $d_E = m_E t_E$ with $m_E = \omega^2 > 0$, so that $\tau_E = \pi/\omega = \pi/\sqrt{m_E}$.

Substituting these values in the matrix exponential of $\mathbf{A}_E$, we get

$$e^{\mathbf{A}_E \tau_E} + \mathbf{I} = \frac{e^{\frac{\pi t_E}{\omega}} + 1}{t_E^2 + \omega^2} \begin{pmatrix} t_E^2 & -t_E & 1 \\ 0 & 0 & 0 \\ t_E^2\omega^2 & -t_E\omega^2 & \omega^2 \end{pmatrix}$$

and from the first component of equation (17), since the kernel of above matrix must contain the vector $(0, 1, v_0)^\top$, we have that

$$-t_E + v_0 = 0,$$

what implies $v_0 = t_E$, and the proof is completed. □

As long as we are in a neighborhood of the solution of (16) studied in Lemma 4, the eigenvalues of $\mathbf{A}_E$ will be a real one λ and a pair of complex numbers $\sigma \pm \omega i$, so that the linear invariants of $\mathbf{A}_E$ can be written as

$$\begin{aligned} t_E &= 2\sigma + \lambda, \\ m_E &= 2\sigma\lambda + \sigma^2 + \omega^2, \\ d_E &= \lambda\left(\sigma^2 + \omega^2\right), \end{aligned} \tag{19}$$

and we see that the quoted solution corresponds with $\sigma = 0$.

The idea is to study the closing equations (16) by looking for the branch of solutions $(r_0, v_0, \tau_E, \tau_C, \sigma)$ with $r_0 > 0$ and positive flight times, that passes through the point $(r_0, v_0, \tau_E, \tau_C, \sigma) = (0, \lambda, \pi/\sqrt{m_E}, 0, 0)$, by varying σ near 0. The interesting points of this branch will satisfy $r_0 > 0$ and $\tau_C > 0$, and will be associated to actual periodic solutions. As it will be shown, it is possible to parameterize the branch of solutions in a local neighborhood of the starting point. This can be done by means of a suitable application of the Implicit Function Theorem.

Now, we are in position to state the main result of this work by studying the solutions of (16) with the conditions given in (19) in a neighborhood of the critical values of Lemma 4. This theorem gives sufficient conditions for system (3) to undergo a Hopf bifurcation from a periodic orbit at infinity, that is, it gives conditions about existence and stability of the limit cycle that bifurcates from infinity.

Theorem 5. *Consider system* (3) *under the assumptions* (19) *with* $\lambda \neq 0$, $\omega > 0$ *and define the non-degeneracy parameter*

$$\rho = d_C - \lambda m_C + \omega^2(\lambda - t_C). \tag{20}$$

If $\rho \neq 0$, *then, for* $\sigma = 0$ *the system undergoes a Hopf bifurcation at infinity, that is, one symmetric limit cycle appears for* $\rho\sigma > 0$ *and* σ *sufficiently small. In particular, if* $\rho < 0$ *and* $\lambda < 0$, *then the limit cycle bifurcates for* $\sigma < 0$ *and is orbitally asymptotically stable. Otherwise, if* $\rho > 0$ *or* $\lambda > 0$ *the bifurcating limit cycle is unstable, being completely unstable when both inequalities hold, see Figure 2.*

Moreover, introducing the constant $\kappa = \exp(\pi\lambda/\omega)$*, the period* P *of the periodic oscillation is an analytic function at* 0*, in the variable* σ*, and its series expansion is*

$$P = \frac{2\pi}{\omega} - \frac{2\pi\left[\lambda\rho + \left(\lambda^2+\omega^2\right)\left(m_C-\omega^2\right)\right]}{\omega^3\rho}\sigma + \frac{\pi\left[A_1\left(1+\kappa\right)+B_1\pi\left(1-\kappa\right)\right]}{\lambda\omega^5\rho^3\left(\kappa+1\right)}\sigma^2 + O\left(\sigma^3\right),$$

where coefficients A_1 *and* B_1 *are given in Table A.1 of Appendix A. The amplitude* a *(measured as* $y_0 = 1/r_0$*) has the following series expansion,*

$$a = \frac{2\omega\rho}{\pi(\lambda^2+\omega^2)\sigma} + \frac{A_2\left(1+\kappa\right)+B_2\pi\left(1-\kappa\right)-2\pi\kappa\lambda^2\rho\omega\left(\lambda^2+\omega^2\right)^2}{\pi\lambda\omega\rho\left(\kappa+1\right)\left(\lambda^2+\omega^2\right)^2} + O\left(\sigma\right),$$

where the coefficients A_2 *and* B_2 *are given in Table A.1 of Appendix A.*

This theorem is in agreement with the results obtained in [15] with different techniques, but gives more quantitative information, see Section 4. For a proof of Theorem 5 see Section 5.

If we introduce the auxiliary parameter

$$\varepsilon = m_E t_E - d_E \tag{21}$$

and consider some critical values m_E^*, t_E^*, d_E^* for the linear invariants of matrix $\mathbf{A}_E$, such that $m_E^* t_E^* = d_E^*$ with $m_E^* > 0$, it is immediate to see that in a neighborhood of such critical values all the conditions (19) are generically fulfilled. Effectively, in such a case we have that the characteristic polynomial of $\mathbf{A}_E$ is

$$\lambda^3 - t_E^*\lambda^2 + m_E^*\lambda - t_E^* m_E^* = (\lambda - t_E^*)(\lambda^2 + m_E^*)$$

so that the eigenvalues of $\mathbf{A}_E$ are t_E^* and $\pm\sqrt{m_E^*}i$. Therefore, we see that for near values, conditions (19) are true and furthermore we have

$$\varepsilon = m_E t_E - d_E = 2\sigma\left[(\sigma+\lambda)^2+\omega^2\right],$$

so that $\text{sign}(\varepsilon) = \text{sign}(\sigma)$. Thus, we can conclude the following corollary, which is a direct consequence of Theorem 5.

Corollary 6. *Consider system* (3) *with* $d_E^* \neq 0$, $m_E^* > 0$, $m_E^* t_E^* = d_E^*$ *and define the parameter* ε *as in* (21) *for* (m_E, t_E, d_E) *in a neighborhood of the critical values* (m_E^*, t_E^*, d_E^*). *Under the non-degeneracy condition*

$$\rho = d_C - t_E^* m_C + m_E^*(t_E^* - t_C) \neq 0 \tag{22}$$

then for $\varepsilon = 0$ *the system undergoes a Hopf bifurcation at infinity, that is, one symmetric limit cycle appears for* $\rho\varepsilon > 0$ *and* ε *sufficiently small. In particular, if* $\rho < 0$ *and* $d_E^* < 0$, *then the limit cycle bifurcates for* $\varepsilon < 0$ *and is orbitally asymptotically stable. Otherwise, if* $\rho > 0$ *or* $d_E^* > 0$ *the bifurcating limit cycle is unstable, being completely unstable when both inequalities hold.*

Regarding Figure 2, we see that the character of the predicted bifurcation from infinity at the axis $\varepsilon = 0$ changes depending on the sign of the criticality parameter ρ. This suggests that the point $(\rho, \varepsilon) = (0, 0)$ is a higher codimension bifurcation point. From such point there could emerge one or more bifurcation curves. Therefore, it is clear that the bifurcation sets of Figure 2 have to be completed; for sake of brevity, we relegate such analysis to a future work.

The rest of the paper is organized as follows. Next, in Section 3 we present an interesting application of Theorem 5, whose proof is offered in Section

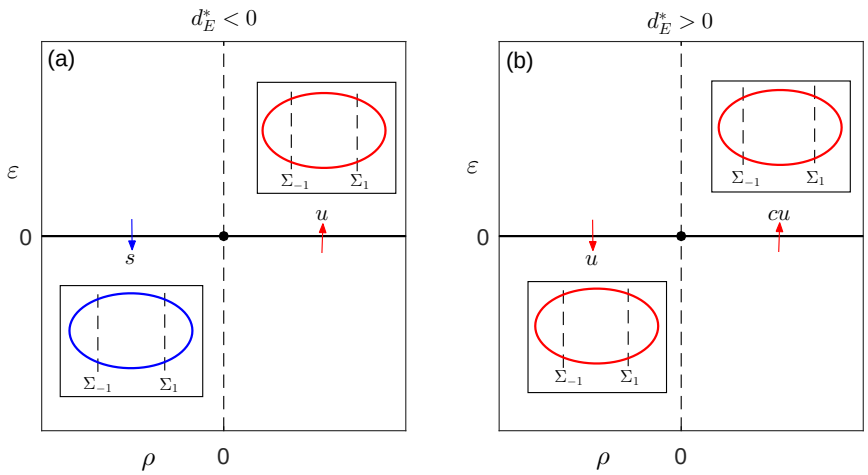

Figure 2: The bifurcations predicted by Corollary 6 in the parameter plane (ρ, ε) under hypotheses $d_E^* < 0$ (left) and $d_E^* > 0$ (right). The arrows indicate the direction of the appearance of the bifurcating stable (s), unstable (u), or completely unstable (cu) limit cycle.

5. In Section 4, we compare our results with those obtained with different techniques in [15]. Finally, the somehow cumbersome proof of Proposition 1 is relegated to Appendix A for ease of reading.

3. Application to a Bonhoeffer-van der Pol oscillator.

In this section we consider an extended Bonhoeffer-van der Pol (BVP) oscillator, which consists of two capacitors, an inductor, a linear resistor and a nonlinear conductance, as shown in Figure 3. More information about this circuit can be found in [37], where a smooth nonlinearity is assumed for the conductance and a rich variety of dynamical behaviors is numerically and experimentally demonstrated. For the purposes of this work, we emphasize

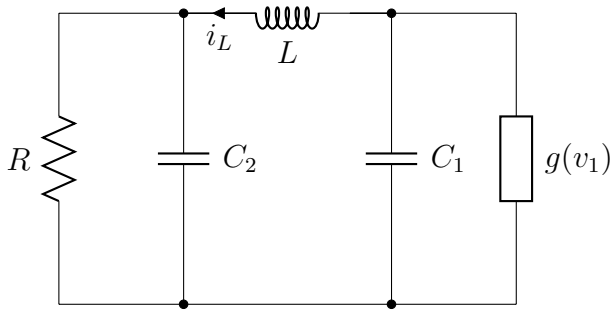

Figure 3: The extended BVP oscillator proposed in [37], where the voltages across the capacitors C_1 and C_2 are v_1 and v_2 respectively.

that in some significant region of the parameter space there was detected one stable oscillation of big amplitude.

The circuit equations are the following:

$$C\frac{dv_1}{dt} = -i_L - g(v_1), \quad C\frac{dv_2}{dt} = i_L - \frac{v_2}{R}, \quad L\frac{di_L}{dt} = v_1 - v_2,$$

where v_1 and v_2 are the voltages across the capacitors C_1 and C_2 respectively, and i_L stands for the current through the inductance L. Note that we take $C_1 = C_2 = C$, and the $v - i$ characteristics of the nonlinear resistor is written as $g(v) = -av - b\,\mathrm{sat}(cv)$, where $a, b, c > 0$. Therefore, we assume a piecewise linear version of the nonlinearity considered in [37], since such assumption is a very good approximation of the actual nonlinear characteristics.

After some standard manipulations, the normalized equations of the extended BVP oscillator are given by

$$\begin{aligned} \dot{x} &= -z + \alpha x + \mathrm{sat}(\beta x), \\ \dot{y} &= z - \delta y, \\ \dot{z} &= x - y, \end{aligned} \tag{23}$$

where the dot represents derivative with respect to the new time τ,

$$\tau = \frac{1}{\sqrt{LC}}t, \quad \alpha = a\sqrt{\frac{L}{C}}, \quad \beta = bc\sqrt{\frac{L}{C}}, \quad \delta = \frac{1}{R}\sqrt{\frac{L}{C}},$$

being α, β, δ positive adimensional parameters, and

$$x = \frac{v_1}{b}\sqrt{\frac{C}{L}}, \quad y = \frac{v_2}{b}\sqrt{\frac{C}{L}}, \quad z = \frac{i_L}{b},$$

the new dimensionless variables.

System (23) can be rewritten into the generalized Liénard form (3), as follows

$$\dot{\mathbf{x}} = \begin{pmatrix} t_E & -1 & 0 \\ m_E & 0 & -1 \\ d_E & 0 & 0 \end{pmatrix} \mathbf{x} + \begin{pmatrix} t_C - t_E \\ m_C - m_E \\ d_C - d_E \end{pmatrix} \operatorname{sat}\left(\mathbf{e}_1^\top \mathbf{x}\right), \tag{24}$$

where the linear invariants are

$$\begin{aligned} &t_C = \alpha - \delta + \beta, \quad m_C = 2 - \delta(\alpha + \beta), \quad d_C = \alpha - \delta + \beta, \\ &t_E = \alpha - \delta, \quad m_E = 2 - \alpha\delta, \quad d_E = \alpha - \delta. \end{aligned} \tag{25}$$

We start by giving some basic information about possible equilibria of the system. The origin is always an equilibrium point and that, from the first component of (6), we have an extra symmetric pair of real equilibria whenever $d_C d_E < 0$, and due to the positiveness of parameters α, β and δ, such inequality is equivalent to the condition

$$\alpha < \delta < \alpha + \beta, \tag{26}$$

which corresponds to region II of the parameter plane in Figure 4(a). Thus, while for $\alpha > \delta$ or $\alpha + \beta < \delta$ there is only one equilibrium at the origin, we pass to have three equilibria in crossing the line $\alpha + \beta = \delta$ (degenerate

pitchfork bifurcation at the origin) or in crossing the line $\alpha = \delta$ (pitchfork bifurcation at infinity). The origin is the only equilibrium point and is stable whenever $\alpha + \beta < 1/\delta$, which corresponds to region I of the parameter plane in Figure 4(a).

It will be assumed for δ a fixed value $\delta^* > 1$, as in [37], and we will study the possible existence of a Hopf bifurcation at infinity that could explain the presence of big stable oscillations for certain parameter values. To this end, we will apply Corollary 6.

We start by seeing that $\varepsilon = (\alpha - \delta^*)(1 - \alpha\delta^*)$, and recalling that the bifurcation appears when such a parameter vanishes. However, as $d_E = \alpha - \delta^* \neq 0$ is a nondegeneracy condition for the bifurcation, we will assume that only the second factor can vanish; that is, our parameters are in a neighborhood of a critical value (m_E^*, t_E^*, d_E^*) with $\alpha^* = 1/\delta^* < 1$, so that $t_E^* = d_E^* < 0$, since $\delta^* > 1$. Note that $m_E^* = 1$ and so all the initial hypotheses in Corollary 6 are fulfilled. For the criticality coefficient ρ, we have from (22) that

$$\rho = \alpha^* - \delta^* - \left[2 - \delta^* \left(\alpha^* + \beta\right)\right] \left(\alpha^* - \delta^*\right) = \left(1 - \frac{1}{\alpha^{*2}}\right) \beta < 0.$$

As a direct consequence of Corollary 6 we get the following result.

Proposition 7. *Consider system* (23) *with δ fixed to a certain value $\delta^* > 1$, and $\alpha > 0$ in a sufficiently small neighborhood of $\alpha^* = 1/\delta^* < 1$. For $\alpha = \alpha^*$ the system undergoes a Hopf bifurcation from a periodic orbit at infinity, that is, one symmetric and orbitally asymptotically stable limit cycle appears for $\alpha^* - \alpha > 0$ and sufficiently small.*

It should be remarked that the bifurcation predicted by Proposition 7,

which could be difficult to be observed in practice, deserves to be understood because it gives a proper explanation for certain 'big' periodic orbits that appear in these circuits, far enough from other possible attractors (see for instance [19, 22]).

We show in Figure 4(a) a partial bifurcation set in the parameter plane (α,β) for fixed $\delta = 6/5$, the same value that was considered in [37], but drawing only the main bifurcation lines that can be analytically justified, and omitting other secondary bifurcation curves that could be numerically detected. We emphasize the vertical line $\alpha = 1/\delta$, denoted by H^{∞}_{PWL}, where the system undergoes a Hopf bifurcation at infinity, according to Proposition 7, which was a missing bifurcation line in the bifurcation sets given in [37]. The vertical line $\alpha = \delta$, denoted by HZ^{E}_{PWL}, represents a Hopf-Zero singularity for the external linearization matrices, leading in particular to a pitchfork bifurcation at infinity for equilibria. There appear other two straight lines of bifurcation points related to the linear part at the central zone, namely he focus-center-limit cycle bifurcation line $\alpha + \beta = 1/\delta$, denoted by H^{C}_{PWL} and analyzed in [26], and the Hopf-Zero bifurcation line $\alpha + \beta = \delta$ studied in [38], denoted by HZ^{C}_{PWL}. Following for $\beta = 3/5$ the path from $\alpha = 7/30$ to $\alpha = 6/5$ we observe, in Figure 4(b) how the value of y_0 evolves from $\alpha_1 = 3/5$ growing and growing, and tending to infinity near the curve $\alpha = 1/\delta$. By computing Poincaré map on the plane $x = 1$, fixing the parameters $\delta = 1.2$, $\beta = 0.3$ and taking α as the bifurcation parameter of system (23), we obtain for the coordinate y_0 the numerical bifurcation diagram given in 4(c), that corresponds to the blue horizontal segment on two-parameter plane $\alpha \times \beta$ showed in Figure 4(a). The bifurcation diagram shows the presence of peri-

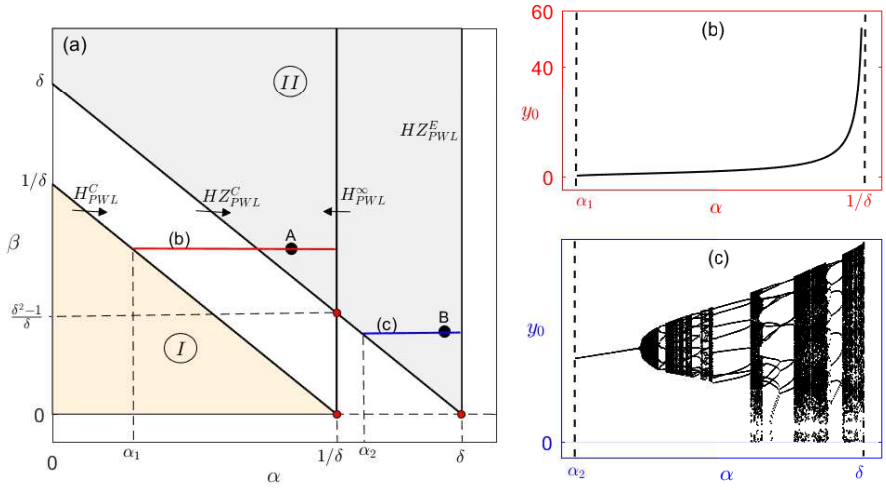

Figure 4: **(a)** Partial bifurcation set in the plane (α, β) for fixed $\delta = 1.2$. At the vertical line $\alpha = 1/\delta$, denoted by H^{∞}_{PWL}, a stable limit cycle comes from (or goes to) infinity. The other vertical line $\alpha = \delta$, denoted by HZ^{E}_{PWL}, represents a pitchfork bifurcation at infinity of equilibria. In region I there is only one stable equilibrium at the origin, while in region II there are three equilibria being stable the external ones. **(b)** Continuation for $\beta = 0.6$ and $\alpha_1 = 0.6$ of the limit cycle generated in the BVP oscillator from the focus-center-limit cycle bifurcation (H^{C}_{PWL}) to the Hopf bifurcation at Infinity (H^{∞}_{PWL}) that occurs at $\alpha = 1/\delta = 5/6$, following the red horizontal segment on the panel (a). We see how the value of y_0 for the intersection point of the orbit with the plane $x = 1$ grows with α and tends to infinity when α tends to $1/\delta = 5/6$. **(c)** Following the blue horizontal segment on the panel (a), fixing $\beta = 0.3$ and taking the coordinate y_0 at the Poincaré section $x = 1$, we show a bifurcation diagram varying parameter α in the interval (α_2, δ) where $\alpha_2 = 1.03$.

odic windows that alternate with strange attractors (quasiperiodicity) that are apparently not chaotic, see Figure 5(b). We also remark that the partial bifurcation set of Figure 4(a) is not complete; we can anticipate the existence of some additional bifurcation curves emanating from the higher codimension
315 points $(1/\delta, (\delta^2-1)/\delta)$, $(1/\delta, 0)$ and $(\delta, 0)$, see the red points in Figure 4(a). A further analysis will appear elsewhere.

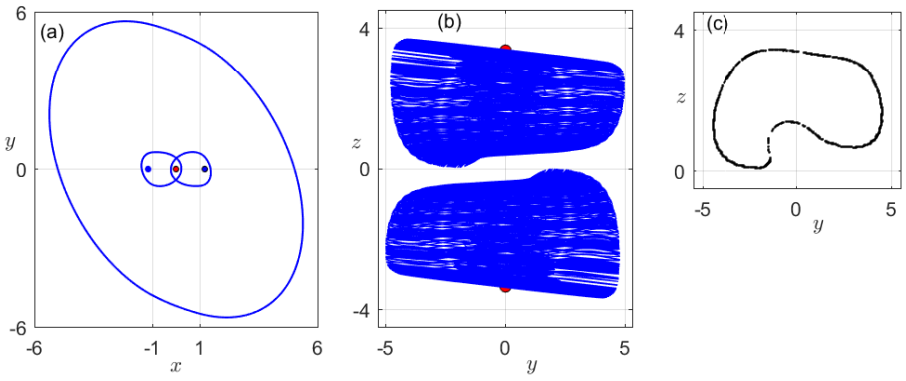

Figure 5: **(a)** For the point A of Figure 4(a), with $\alpha = 1.2$ and $\beta = 0.6$, we show three stable limit cycles that coexist with two stable equilibria. The appearance of both the new equilibria symmetric and the two bi-zonal limit cycles, along with other unstable limit cycles not shown in the picture, can be explained via a Hopf-Zero bifurcation (HZ^C_{PWL}). If we increase the value of α until it approaches $\alpha = 1/\delta = 5/6$ then the stable limit cycle grows to disappear in the Hopf bifurcation at infinity H^{∞}_{PWL}. **(b)** For the point B of Figure 4(a), with $\alpha = 1.15$ and $\beta = 0.3$, we show two stable symmetrical strange attractors. **(c)** The Poincaré section at $x = 1$ for the upper stable symmetrical strange attractor shown in panel (b).

Figure 5(a) shows that system (23) exhibits a dynamic behavior of multiple attractors for the parameters $\delta = 1.2$, $\alpha = 1.2$ and $\beta = 0.6$, that is, the systems has three stable limit cycles that coexist with two stable equilibria.

In Figure 4(b), we show for the parameters $\delta = 1.2$, $\alpha = 1.15$ and $\beta = 0.3$ (the point B of Figure 4(a)) the phase portrait of the two strange symmetric attractors that are apparently not chaotic (for more details see [39]). This dynamical behavior coincides with the presence of quasiperiodicity that was reported numerically in [37], where the nonlinearity $g(v)$ of the extended BVP oscillator was considerer as a smooth function.

A final remark is in order. If under hypotheses of Proposition 7, condition (26) holds for the critical values of parameters, then it should be remarked that at $\alpha = 1/\delta^*$ the additional equilibria undergo the so called focus-center-limit cycle bifurcation studied in [24], leading to a symmetric pair of non symmetric limit cycles. Therefore, under hypotheses of Proposition 7, there could appear more than one limit cycle. This simultaneous bifurcation of limit cycles, one of them coming from infinity will be studied elsewhere.

4. Comparison with a previous analysis

In [15], a Hopf bifurcation at infinity is analyzed for the class of control systems with a bounded nonlinearity asymptotically homogeneous at infinity. While the required hypotheses for the nonlinearity in the results in [15] are weaker than the ones in Theorem 5, some other related with the linear part at infinity are more restrictive. They consider systems of the form

$$\frac{d\mathbf{z}}{dt} = \mathbf{A}(\mu)\mathbf{z} + \gamma(\mu)f(x(t))), \quad x(t) = \mathbf{c}^\top \mathbf{z}(t) \tag{27}$$

where the scalar nonlinearity f and the matrix $\mathbf{A}(\mu)$ satisfy the following properties.

(i) There exist finite limits $f_- = \lim_{x\to-\infty} f(x)$, $f_+ = \lim_{x\to\infty} f(x)$ and $f_- \neq f_+$.

(ii) The function f is globally Lipschitz continuous and moreover

$$|f(x_1) - f(x_2)| \leq \alpha(r)|x_1 - x_2|, \quad |x_1|, |x_2| \geq r, \quad x_1 x_2 > 0,$$

where $\alpha(r) = o(r^{-1}),\ r \to \infty$.

(iii) The numbers $\sigma(\mu) \pm i\omega(\mu)$ are simple eigenvalues of $\mathbf{A}(\mu)$, where $\sigma(\mu_0) = 0$, $\omega(\mu_0) = 0$ and every other eigenvalue has negative real part.

(iv) The inequality $\mathbf{c}^\top \mathbf{P}_E \gamma(\mu_0) \neq 0$ holds, where $\mathbf{P}_E$ is the projection matrix onto the two dimensional invariant subspace E of the matrix $\mathbf{A}(\mu_0)$, following the direction of its complementary invariant subspace E'.

In [15] the following result was proven.

Theorem 8. *Under hypotheses (i)-(iv), after introducing the criticality coefficient*

$$\eta = 2(f_+ - f_-)\mathbf{c}^\top \mathbf{P}_E \gamma(\mu_0) \tag{28}$$

and the sets

$$M_+^\delta = \mu : \sigma(\mu)\eta \geq 0, \quad |\mu - \mu_0| < \delta, \tag{29}$$

$$M_-^\delta = \mu : \sigma(\mu)\eta < 0, \quad |\mu - \mu_0| < \delta, \tag{30}$$

the following statements hold.

There exist $r_0 > 0$ and $\delta > 0$ such that system (3) has no r_0-large periodic cycles whenever $\mu \in M_+^\delta$. System (3) has a unique r_0-large periodic cycle $\mathbf{z}_*(t, \mu)$ for every $\mu \in M_-^\delta$. The cycle $\mathbf{z}_*(t, \mu)$ depends continuously on μ and $\|\mathbf{z}_*(\cdot, \mu)\| \to \infty$ as $\mu \to \mu_0,\ \mu \in M_-^\delta$, being orbitally asymptotically stable if $\eta > 0$ and orbitaly unstable if $\eta < 0$.

Since system (3) is endowed with a bounded nonlinearity (the saturation function) that fulfills all the required hypotheses, it seems interesting to compare our results with the predicted ones by Theorem 8. Clearly, for system (3), as $f(x) = \mathrm{sat}(x)$, we have $f_- = -1$, $f_+ = 1$, and (i), (ii) are trivially satisfied with $\alpha(r) \equiv 0$. Hypothesis (iii) is included in the hypotheses of Theorem 5 (but note we only require $\lambda \neq 0$ and not $\lambda < 0$). To compute the matrix $\mathbf{P}_E$, it suffices to take a left eigenvector of $\mathbf{A}_E$ for $\sigma = 0$, namely $\mathbf{w}_0^\top = (\lambda^2, -\lambda, 1)$ so that $E = \{(x, y, z) : \lambda^2 x - \lambda y + z = 0\}$, and to derive the corresponding projection matrix, following the direction of the complementary invariant subspace $E' = \{(x, y, z) : y = 0, \quad z = \omega^2 x\}$. Taking the vector $\mathbf{v}_0^\top = (1, 0, \omega^2)^\top$ as generator of E', we have

$$\mathbf{P}_{E'} = \frac{\mathbf{v}_0 \mathbf{w}_0^\top}{\mathbf{w}_0^\top \mathbf{v}_0} = \frac{1}{\lambda^2 + \omega^2} \begin{pmatrix} \lambda^2 & -\lambda & 1 \\ 0 & 0 & 0 \\ \lambda^2\omega^2 & -\lambda\omega^2 & \omega^2 \end{pmatrix},$$

so that

$$\mathbf{P}_E = \mathbf{I} - \frac{\mathbf{v}_0 \mathbf{w}_0^\top}{\mathbf{w}_0^\top \mathbf{v}_0} = \frac{1}{\lambda^2 + \omega^2} \begin{pmatrix} \omega^2 & \lambda & -1 \\ 0 & 1 & 0 \\ -\lambda^2\omega^2 & \lambda\omega^2 & \lambda^2 \end{pmatrix}.$$

Finally, noting that $\mathbf{c}^\top = \mathbf{e}_1^\top$ and that $\gamma(\mu_0)$ is the vector in the non-homogeneous part of (3) for $t_E = t_E^* = \lambda$, $m_E = m_E^* = \omega^2$ and $d_E = d_E^* = \lambda\omega^2$, that is $\gamma(\mu_0) = (t_C - \lambda, m_C - \omega^2, d_C - \lambda\omega^2)^\top$, we obtain

$$\eta = 4\mathbf{e}_1^\top \mathbf{P}_E \mathbf{b} = \frac{4}{\lambda^2 + \omega^2}[\omega^2(t_C - \lambda) + \lambda(m_C - \omega^2) - (d_C - \lambda\omega^2)],$$

and after substituting the value (22) and simplifying, it results

$$\eta = -\frac{4\rho}{\lambda^2 + \omega^2},$$

equality that establishes the relationship between coefficients η and ρ. Thus, we conclude that our results are in agreement with [15]. Note however, that as we are working with a specific family of piecewise linear systems, we obtain much more information that in the quoted study.

5. Proof of Theorem 5

We proceed by studying the closing equations (16) looking for the solutions, with small r_0 that can bifurcate from the critical solution of Lemma 4. Assuming λ and ω fixed for the configuration of eigenvalues (19), we have a set of four equations in five variables, to be denoted by

$$\mathbf{F}(\mathbf{z}) = \mathbf{0}, \tag{31}$$

where $\mathbf{z} = (r_0, v_0, \tau_E, \tau_C, \sigma)$, to be analyzed in a neighborhood of the critical point $\bar{\mathbf{z}} = (0, \lambda, \pi/\omega, 0, 0)$, via a straightforward application of the Implicit Function Theorem. We note that to evaluate the left hand side in (31) or equivalently (16) we need to compute some matrix exponentials, namely $\exp(\mathbf{A}_C\tau_C)$ and $\exp(-\mathbf{A}_E\tau_E)$. While from (19) we can explicitly compute the last one, for the first one we resort to the expansion

$$e^{\mathbf{A}_C\tau_C} = \mathbf{I} + \mathbf{A}_C\tau_C + \frac{\mathbf{A}_C^2\tau_C^2}{2!} + \cdots .$$

Our first auxiliary result is the following.

Lemma 9. *Under hypotheses* (19) *with* $\lambda \neq 0$ *and* $\omega > 0$*, the point* $\bar{\mathbf{z}}$ *is a regular point of the modified closing equations* (16)*. Consequently, in a neighborhood of* $\bar{\mathbf{z}}$*, there exists only one branch of solutions* $(r_0(\sigma), v_0(\sigma), \tau_E(\sigma), \tau_C(\sigma), \sigma)$*, with the analytic expansions*

$$r_0 = \frac{\pi\left(\lambda^2+\omega^2\right)}{2\omega\rho}\sigma + \frac{\pi\left[A_3(1+\kappa)+B_3\pi(1+\kappa)+2\pi\kappa\lambda^2\rho\omega(\lambda^2+\omega^2)^2\right]}{2\lambda\rho^3\omega^5(1+\kappa)}\sigma^2+O(\sigma^3), \tag{32}$$

$$v_0 = \frac{\pi\left[\lambda\omega^2-\rho-t_C(\lambda^2+\omega^2)+\kappa(\rho+\omega^2(t_C-\lambda)+(\lambda^2(t_C-2\lambda))\right](\lambda^2+\omega^2)}{2\lambda\rho\omega(1+\kappa)}\sigma+ \tag{33}$$

$$+\frac{\pi\left[A_4+B_4\pi+\kappa(A_5+B_5\pi)+\kappa^2(A_6+B_6\pi)\right]}{2\lambda^2\rho^3\omega^4(1+\kappa)^2}\sigma^2+O(\sigma^3), \tag{34}$$

$$\tau_E = -\frac{\pi\left(\lambda\rho+m_C\left(\lambda^2+\omega^2\right)\right)}{\omega^3\rho}\sigma + \frac{\pi\left[A_7(1+\kappa)+B_7\pi(1-\kappa)\right]}{2\lambda\rho^3\omega^5(1+\kappa)}\sigma^2+O(\sigma^3), \tag{35}$$

$$\tau_C = \frac{\pi\left(\lambda^2+\omega^2\right)}{\omega\rho}\sigma + \frac{\pi\left[A_8(1+\kappa)-B_8\pi(1-\kappa)\right]}{2\lambda\rho^3\omega^5(1+\kappa)}\sigma^2+O(\sigma^3), \tag{36}$$

where $\rho = d_C - \lambda m_C + \omega^2(\lambda - t_C)$, $\kappa = \exp(\pi\lambda/\omega)$ *and the expressions* A_i, B_i *with* $i, j = 3, \ldots, 8$ *are shown in Table A.1 of Appendix A.*

Proof. The set of equations (31) is defined by analytic functions near $\bar{\mathbf{z}}$. For the Jacobian matrix, we have

$$D_{\mathbf{z}}\mathbf{F}(\mathbf{z})|_{\bar{\mathbf{z}}} = \begin{pmatrix} 2 & 0 & 0 & -1 & 0 \\ 2+\frac{d_C\left(\omega^2\phi-2\right)}{\lambda\omega^2}+(\lambda t_C - m_C)\phi & \phi & -1 & -1 & 0 \\ 2t_C - \frac{2d_C}{\omega^2} & 0 & -\lambda & -\lambda & \frac{\pi}{\omega} \\ 2m_C+\frac{d_C\left(\omega^2\phi-2\right)}{\lambda}+(\lambda t_C - m_C)\omega^2\phi & \phi & 0 & 0 & \frac{\pi\lambda}{\omega} \end{pmatrix}$$

where

$$\phi = \frac{1+e^{-\frac{\pi\lambda}{\omega}}}{\lambda^2+\omega^2} = \frac{\kappa+1}{\kappa(\lambda^2+\omega^2)} \neq 0.$$

We note that the determinant of the submatrix obtained by removing the last column, which corresponds to σ, is equal to $2\rho\phi \neq 0$, so that the rank of

the Jacobian matrix is 4 and we can apply the Implicit Function Theorem for analytic functions in (31), see [1]. Consequently, the given series expansions $r_0(\sigma)$, $v_0(\sigma)$, $\tau_E(\sigma)$ and $\tau_C(\sigma)$ have been obtained from the closing equations (31) using symbolic computation with [40], and the Lemma follows. □

Remark 10. *From the branch of solutions obtained in Lemma 9, we must only consider the part giving $\tau_C > 0$, that is we need $\rho\sigma > 0$; otherwise, the solution cannot be identified with a periodic orbit of the original system* (3).

According to the above remark, and assuming $\rho\sigma > 0$, we can study the stability of the bifurcating periodic orbits by resorting to Corollary 2. Instead of computing the eigenvalues of such product of matrix exponentials (as done in [26]) we follow here the approach given in [28], which is based in the following elementary results.

Lemma 11. *The two solutions of the equation $x^2 - px + q = 0$, where p, $q \in \mathbb{R}$, are inside the unit circle of the complex plane if and only if $|q| < 1$ and $|p| < 1 + q$.*

Using the above lemma, the following remark will be used to determine the stability of period orbits.

Remark 12. *The matrix $\mathbf{M}$ in* (11) *has one eigenvalue equal to -1. We will denote by λ_1 and λ_2 the other two eigenvalues. Therefore, if we take $p = \lambda_1 + \lambda_2$ and $q = \lambda_1\lambda_2$, we have $\mathrm{trace}(\mathbf{M}) = -1 + p$ and $\det(\mathbf{M}) = -q$, and thus the characteristic equation of matrix $\mathbf{M}$ is $(\lambda+1)(\lambda^2 - p\lambda + q) = 0$. Then λ_1 and λ_2 are the eigenvalues of the derivative $D_{\boldsymbol{p}}\pi_{EC}$, see Proposition 1, and from Lemma 11 both eigenvalues λ_1 and λ_2 are inside the unit circle*

if and only if

$$|\det(\mathbf{M})| < 1 \text{ and } |\operatorname{trace}(\mathbf{M}) + 1| < 1 - \det(\mathbf{M}). \tag{37}$$

Finally, as the eigenvalues of the derivative of the complete Poincaré map are λ_1^2 and λ_2^2, if the conditions (37) *are fulfilled, then we can assure that the corresponding periodic orbit is stable.*

Taking into account the expressions for τ_E and τ_C of Lemma 9, and substituting in (11) we get

$$\operatorname{trace}(\mathbf{M}) = e^{\frac{\pi\lambda}{\omega}} - 2 - \frac{\pi\left[-\rho\omega^2 + e^{\frac{\pi\lambda}{\omega}}\left(\rho\left(\omega^2-\lambda^2\right) + \left(t_C\omega^2 - \lambda m_C\right)\left(\lambda^2+\omega^2\right)\right)\right]}{\omega^3\rho}\sigma + O(\sigma^2),$$

$$\det(\mathbf{M}) = e^{\frac{\pi\lambda}{\omega}} - \frac{\pi e^{\frac{\pi\lambda}{\omega}}}{\omega^3\rho}\left[\rho\left(\lambda^2-2\omega^2\right) + \left(\lambda m_C - t_C\omega^2\right)\left(\lambda^2+\omega^2\right)\right]\sigma + O(\sigma^2).$$

The first condition of (37) is fulfilled for $\lambda < 0$ and σ sufficiently small. Assuming $\lambda < 0$, we get the expression

$$|\operatorname{trace}(\mathbf{M}) + 1| - 1 + \det(\mathbf{M}) = \frac{\pi}{\omega}\left(1 + e^{\frac{\pi\lambda}{\omega}}\right)\sigma + O(\sigma^2),$$

so that the second condition of (37) leads to

$$\frac{\pi}{\omega}\left(1 + e^{\frac{\pi\lambda}{\omega}}\right)\sigma < 0.$$

Therefore, the bifurcating limit cycle is stable for $\lambda < 0$ and $\sigma < 0$. Using now that the bifurcating limit cycle exists for $\sigma\rho > 0$, we obtain the equivalent conditions $\rho < 0$ and $\lambda < 0$ for stability, as stated in Theorem 5.

The expansions of the period and the amplitude of the bifurcating limit cycle are obtained straightforwardly using the series expansions of Lemma 9.

6. Concluding remarks

Bifurcations at infinity are not usually considered in the bifurcation analysis of nonlinear systems. However, in the framework of piecewise linear systems such bifurcations appear in a natural way defining parametric frontiers for the existence of periodic orbits. Thus, our study fills a gap in the relevant case of three-dimensional symmetric continuous piecewise linear systems with three zones, by studying their possible Hopf bifurcations at infinity.

After adapting the so-called closing equations method for making it able to work with periodic orbits of great amplitude (periodic orbits near the point at infinity), we provide a complete characterization of the stability, amplitude and period of the limit cycle that can bifurcate from the point at infinity in the piecewise linear family of systems under study.

Our achievements are compared with previous known results on the Hopf bifurcation at infinity, emphasizing the information gained with the followed approach. The appearance or disappearance of a large amplitude limit cycle in a Bonhoeffer-Van der Pol oscillator, which had been missed in a previous analysis, is reported here as an illustrative example of the usefulness of our work.

7. Acknowledgements

Andrés Amador is supported by *Pontificia Universidad Javeriana Cali-Colombia*. The remaining authors are partially supported by the *Ministerio de Economía y Competitividad*, in the frame of projects MTM2015-65608-P, MTM-2014-56272-C2-1-P and PGC2018-096265-B-I00, and by the *Consejería de Economía y Conocimiento de la Junta de Andalucía* under grant

P12-FQM-1658. The authors declare that there is no conflict of interest regarding the publication of this article.

Appendix A. Proof of Proposition 1

Let be $\mathbf{p}_0$, $\mathbf{p}_1$, $\mathbf{p}_2$, $\mathbf{p}_3 \in \mathbb{R}^2$ the reduced coordinates of intersection points $\mathbf{x}_0$, $\mathbf{x}_1$, $\mathbf{x}_2$, $\mathbf{x}_3$, respectively for a given orbit near a symmetric periodic orbit Γ. The points $\mathbf{x}_1$, $\mathbf{x}_2$ are on the Σ_{-1} while $\mathbf{x}_0$, $\mathbf{x}_3$ are on Σ_1. The first equation of (12) can be written as

$$\mathbf{F}_C(\tau_C, y_1, z_1, y_0, z_0) = e^{\mathbf{A}_C \tau_C} \begin{pmatrix} 1 \\ \mathbf{p}_0 \end{pmatrix} - \begin{pmatrix} -1 \\ \mathbf{p}_1 \end{pmatrix} = \mathbf{0}, \tag{A.1}$$

where $\mathbf{p}_0 = (y_0, z_0)^\top$ and $\mathbf{p}_1 = (y_1, z_1)^\top$. In what follows, we will denote the Jacobian matrix of $\mathbf{F}_C$ respect to (τ_C, y_1, z_1) as

$$\mathbf{B}_1 = \left. \frac{D\mathbf{F}_C(\tau_C, y_1, z_1, y_0, z_0)}{D(\tau_C, y_1, z_1)} \right|_\Gamma,$$

evaluated on the periodic orbit Γ. Recall that we denote with hats the coordinates and flight times corresponding with the involved symmetric periodic orbit. Using the closing equation (12), such matrix turns out to be

$$\mathbf{B}_1 = \left(\begin{array}{c|c} \mathbf{A}_C e^{\mathbf{A}_C \hat{\tau}_C} \hat{\mathbf{x}}_0 & \mathbf{0} \\ & -\mathbf{I}_2 \end{array} \right) = \left(\begin{array}{c|c} \mathbf{A}_C \hat{\mathbf{x}}_1 & \mathbf{0} \\ & -\mathbf{I}_2 \end{array} \right),$$

where $\hat{\mathbf{x}}_0 = (1, \hat{\mathbf{p}}_0)^\top$ and $\hat{\mathbf{x}}_1 = (-1, \hat{\mathbf{p}}_1)^\top$ and its determinant is $\det(\mathbf{B}_1) = -t_C + \hat{y}_1 \neq 0$, due to the transversality of the periodic orbit Γ. Here $\mathbf{I}_2$ represents the identity matrix of order two.

Analogously, in the external zone L we rewrite the second equation of (12) as

$$\mathbf{F}_L(\tau_E, y_0, z_0, y_1, z_1) = e^{\mathbf{A}_E \tau_E} \left[\begin{pmatrix} -1 \\ \mathbf{p}_1 \end{pmatrix} - \overline{\mathbf{x}}_L \right] + \begin{pmatrix} 1 \\ \mathbf{p}_0 \end{pmatrix} + \overline{\mathbf{x}}_L = \mathbf{0}, \quad \text{(A.2)}$$

so that on the periodic orbit Γ, we have $e^{\mathbf{A}_E \hat{\tau}_E} (\hat{\mathbf{x}}_1 - \overline{\mathbf{x}}_L) + \hat{\mathbf{x}}_0 + \overline{\mathbf{x}}_L = \mathbf{0}$, and it is easy to show that

$$\left. \frac{\partial \mathbf{F}_L(\tau_E, y_0, z_0, y_1, z_1)}{\partial \tau_E} \right|_\Gamma = \mathbf{A}_E e^{\mathbf{A}_E \hat{\tau}_E} (\hat{\mathbf{x}}_1 - \overline{\mathbf{x}}_L) = \mathbf{A}_E (\hat{\mathbf{x}}_2 - \overline{\mathbf{x}}_L) = -\mathbf{A}_E \hat{\mathbf{x}}_0 - \mathbf{b},$$

where the symmetry of the periodic orbit ($\hat{\mathbf{x}}_2 = -\hat{\mathbf{x}}_0$) has been used.

The Jacobian matrix of $\mathbf{F}_L$ evaluated on the periodic orbit is computed taking into account the continuity of the vector field, as follows.

$$\mathbf{B}_0 = \left. \frac{D\mathbf{F}_L(\tau_E, y_0, z_0, y_1, z_1)}{D(\tau_E, y_1, z_1)} \right|_\Gamma = \left(\begin{array}{c|c} -\mathbf{A}_E \hat{\mathbf{x}}_0 - \mathbf{b} & \mathbf{0} \\ & -\mathbf{I}_2 \end{array} \right) = \left(\begin{array}{c|c} -\mathbf{A}_C \hat{\mathbf{x}}_0 & \mathbf{0} \\ & -\mathbf{I}_2 \end{array} \right),$$

with determinant $-t_C + \hat{y}_0 \neq 0$ due to the transversality hypothesis.

Applying the Implicit Function Theorem to equation (A.1), we obtain the existence of certain functions $\Psi_1(y_0, z_0)$, $\Psi_2(y_0, z_0)$ and $\Psi_3(y_0, z_0)$, such that, in an open neighborhood of the point $\hat{\mathbf{p}}_0 = (\hat{y}_0, \hat{z}_0)$, we have

$$\mathbf{F}_C \left(\Psi_1(y_0, z_0), \Psi_2(y_0, z_0), \Psi_3(y_0, z_0), y_0, z_0 \right) = \mathbf{0},$$

that is, $\tau_C = \Psi_1(y_0, z_0)$, $\mathbf{p}_1 = [\Psi_2(y_0, z_0), \Psi_3(y_0, z_0)]^\top$. Taking implicit derivatives in equation (A.1) respect to variables y_0, z_0, we obtain the following equations

$$\frac{\partial \mathbf{F}_C(\tau_C, y_1, z_1, y_0, z_0)}{\partial y_0} + \frac{D\mathbf{F}_C(\tau_C, y_1, z_1, y_0, z_0)}{D(\tau_C, \mathbf{p}_1)} \left(\begin{array}{ccc} \frac{\partial \Psi_1}{\partial y_0}, & \frac{\partial \Psi_2}{\partial y_0}, & \frac{\partial \Psi_3}{\partial y_0} \end{array} \right)^\top = \mathbf{0},$$

$$\frac{\partial \mathbf{F}_C(\tau_C, y_1, z_1, y_0, z_0)}{\partial z_0} + \frac{D\mathbf{F}_C(\tau_C, y_1, z_1, y_0, z_0)}{D(\tau_C, \mathbf{p}_1)} \left(\begin{array}{ccc} \frac{\partial \Psi_1}{\partial z_0}, & \frac{\partial \Psi_2}{\partial z_0}, & \frac{\partial \Psi_3}{\partial z_0} \end{array} \right)^\top = \mathbf{0},$$

which after being evaluated on the periodic orbit Γ, they can be rewriten as

$$\left.\frac{D\mathbf{F}_C(\tau_C, y_1, z_1, y_0, z_0)}{D(y_0, z_0)}\right|_\Gamma + \left.\frac{D\mathbf{F}_C(\tau_C, y_1, z_1, y_0, z_0)}{D(\tau_C, y_1, z_1)}\right|_\Gamma \left.\begin{pmatrix} \frac{\partial\Psi_1}{\partial y_0} & \frac{\partial\Psi_1}{\partial z_0} \\ \frac{\partial\Psi_2}{\partial y_0} & \frac{\partial\Psi_2}{\partial z_0} \\ \frac{\partial\Psi_3}{\partial y_0} & \frac{\partial\Psi_3}{\partial z_0} \end{pmatrix}\right|_\Gamma = \mathbf{0}.$$

From (A.1) and taking into account that $\pi_C(\hat{\mathbf{p}}_0) = \hat{\mathbf{p}}_1$ on the periodic orbit Γ, we obtain the equivalent equation

$$\mathbf{B}_1 \begin{pmatrix} D_{\mathbf{p}}\tau_C(\hat{\mathbf{p}}_0) \\ D_{\mathbf{p}}\pi_C(\hat{\mathbf{p}}_0) \end{pmatrix} = e^{\mathbf{A}_C\hat{\tau}_C} \left(\begin{array}{c|c} 0 & 0 \\ -1 & 0 \\ 0 & -1 \end{array}\right).$$

Since

$$\mathbf{B}_1 \begin{pmatrix} -1 \\ 0 \\ 0 \end{pmatrix} = -\mathbf{A}_C e^{\mathbf{A}_C\hat{\tau}_C}\hat{\mathbf{x}}_0,$$

we finally obtain

$$\mathbf{B}_1\mathbf{Q}_C = e^{\mathbf{A}_C\hat{\tau}_C}\mathbf{B}_0, \tag{A.3}$$

where

$$\mathbf{Q}_C = \begin{pmatrix} -1 & D_{\mathbf{p}}\tau_C(\hat{\mathbf{p}}_0) \\ \mathbf{0} & D_{\mathbf{p}}\pi_C(\hat{\mathbf{p}}_0) \end{pmatrix}.$$

In what follows, an analogous analysis for the equations of zone L is done. Using again the transversality hypothesis we can apply the Implicit Function Theorem to equation (A.2) and obtain the existence of some functions $\Phi_1(y_1, z_1)$ and $\Phi_2(y_1, z_1)$, such that, in an open neighborhood of the

point $\hat{\mathbf{p}}_1 = (\hat{y}_1, \hat{z}_1)$, satisfy

$$\mathbf{F}_L\left(\Phi_1(y_1, z_1), \Phi_2(y_1, z_1), \Phi_3(y_1, z_1), y_1, z_1\right) = \mathbf{0}, \tag{A.4}$$

with $\tau_L = \Phi_1(y_1, z_1)$, $y_0 = \Phi_2(y_1, z_1)$ and $z_0 = \Phi_3(y_1, z_1)$.

Taking implicit derivatives of equation (A.4) respect to variables y_1 and z_1, we obtain the following equations

$$\frac{\partial \mathbf{F}_L(\tau_L, y_0, z_0, y_1, z_1)}{\partial y_1} + \frac{D\mathbf{F}_L(\tau_L, y_0, z_0, y_1, z_1)}{D(\tau_L, y_0, z_0)} \begin{pmatrix} \dfrac{\partial \Phi_1}{\partial y_1}, & \dfrac{\partial \Phi_2}{\partial y_1}, & \dfrac{\partial \Phi_3}{\partial y_1} \end{pmatrix}^\top = \mathbf{0},$$
$$\frac{\partial \mathbf{F}_L(\tau_L, y_0, z_0, y_1, z_1)}{\partial z_1} + \frac{D\mathbf{F}_L(\tau_L, y_0, z_0, y_1, z_1)}{D(\tau_L, y_0, z_0)} \begin{pmatrix} \dfrac{\partial \Phi_1}{\partial z_1}, & \dfrac{\partial \Phi_2}{\partial z_1}, & \dfrac{\partial \Phi_3}{\partial z_1} \end{pmatrix}^\top = \mathbf{0}.$$

Evaluating these equations on the periodic orbit Γ we obtain

$$\frac{D\mathbf{F}_L(\tau_L, y_0, z_0, y_1, z_1)}{D(y_0, z_0)}\bigg|_\Gamma + \frac{D\mathbf{F}_L(\tau_L, y_0, z_0, y_1, z_1)}{D(\tau_L, y_0, z_0)}\bigg|_\Gamma \begin{pmatrix} \dfrac{\partial \Phi_1}{\partial y_1} & \dfrac{\partial \Phi_1}{\partial z_1} \\ \dfrac{\partial \Phi_2}{\partial y_1} & \dfrac{\partial \Phi_2}{\partial z_1} \\ \dfrac{\partial \Phi_3}{\partial y_1} & \dfrac{\partial \Phi_3}{\partial z_1} \end{pmatrix}_\Gamma = \mathbf{0}.$$

Since $\pi_L(\hat{\mathbf{p}}_1) = \hat{\mathbf{p}}_2 = -\hat{\mathbf{p}}_0$ on the periodic orbit, we have

$$\mathbf{B}_0 \begin{pmatrix} D_{\mathbf{p}}\tau_L(\hat{\mathbf{p}}_1) \\ D_{\mathbf{p}}\pi_L(\hat{\mathbf{p}}_1) \end{pmatrix} = e^{\mathbf{A}_E \hat{\tau}_E} \left(\begin{array}{c|c} 0 & 0 \\ -1 & 0 \\ 0 & -1 \end{array}\right).$$

From equation (A.2) and using the continuity of the vector field, we see that

$$-\mathbf{A}_C \hat{\mathbf{x}}_0 \;\; = -\mathbf{A}_E \hat{\mathbf{x}}_0 - \mathbf{b} = \mathbf{A}_E \left[\hat{\mathbf{x}}_L + e^{\mathbf{A}_E \hat{\tau}_E}\left(\hat{\mathbf{x}}_1 - \overline{\mathbf{x}}_L\right)\right] - \mathbf{b} =$$

$$= e^{\mathbf{A}_E \hat{\tau}_E} \mathbf{A}_E \left(\hat{\mathbf{x}}_1 - \overline{\mathbf{x}}_L\right) = e^{\mathbf{A}_E \hat{\tau}_E}\left(\mathbf{A}_E \hat{\mathbf{x}}_1 - \mathbf{b}\right) = e^{\mathbf{A}_E \hat{\tau}_E} \mathbf{A}_C \hat{\mathbf{x}}_1,$$

Therefore, we conclude that

$$\mathbf{B}_0 \begin{pmatrix} 1 \\ 0 \\ 0 \end{pmatrix} = -\mathbf{A}_C \hat{\mathbf{x}}_0 = e^{\mathbf{A}_E \hat{\tau}_E} \mathbf{A}_C \hat{\mathbf{x}}_1,$$

so that

$$\mathbf{B}_0 \mathbf{Q}_L = e^{\mathbf{A}_E \hat{\tau}_E} \mathbf{B}_1, \tag{A.5}$$

where

$$\mathbf{Q}_L = \begin{pmatrix} 1 & D_{\mathbf{p}} \tau_E(\mathbf{p}_1) \\ \mathbf{0} & D_{\mathbf{p}} \pi_E(\mathbf{p}_1) \end{pmatrix}.$$

Multiplying (A.3) by $e^{\mathbf{A}_E \hat{\tau}_E}$ and taking into account (A.5), we finally have

$$e^{\mathbf{A}_E \hat{\tau}_E} e^{\mathbf{A}_C \hat{\tau}_C} \mathbf{B}_0 = e^{\mathbf{A}_L \hat{\tau}_L} \mathbf{B}_1 \mathbf{Q}_C = \mathbf{B}_0 \mathbf{Q}_L \mathbf{Q}_C,$$

where $\mathbf{B}_0$ is non-singular. The proposition is shown.

$A_1 = 4\lambda\rho\left[\lambda^2\rho^2 + \lambda^4 m_C^2 + 2\lambda^3 m_C\rho + \omega^2\left(-2\lambda^3\rho + 2\lambda^2 m_C^2 - 2\lambda^4 m_C + 3\lambda m_C\rho + \lambda^3 m_C t_C + \rho^2 + \lambda^2\rho t_C\right)\right] +$ $+4\lambda\rho\left[\omega^4\left(\lambda^4 - 3\lambda\rho + m_C^2 - 3\lambda^2 m_C + \lambda m_C t_C - \lambda^3 t_C + \rho t_C\right) + \omega^6\left(\lambda^2 - m_C - \lambda m_C\right)\right]$
$B_1 = \omega\left(\lambda^2+\omega^2\right)\left[\lambda^2\omega^4 - 2\lambda\rho\omega^2 + m_C^2\left(\lambda^2+\omega^2\right) - 2m_C\left(\lambda^2\omega^2 - \lambda\rho + \omega^4\right) + \rho^2 + \omega^6\right]\left[-\lambda^3 - \lambda\omega^2 + \rho + t_C\left(\lambda^2+\omega^2\right)\right]$
$A_2 = 4\lambda\rho\left\{m_C\left(\lambda^2+\omega^2\right)^2 + \lambda\left[-\lambda^3\omega^2 - \lambda\omega^4 + 2\rho\omega^2 + \lambda^2\left(\rho + t_C\omega^2\right) + t_C\omega^4\right]\right\}$
$B_2 = \omega\left(\lambda^2+\omega^2\right)\left\{-\rho\omega^4 + \lambda^5\omega^2 - \lambda^4\rho + 2\lambda^3\omega^4 - 2\lambda^2\rho\omega^2 + 2\lambda\rho^2 + \lambda\omega^6 + m_C\left(\lambda^2+\omega^2\right)\left[-\lambda^3 - \lambda\omega^2 + \rho + t_C\left(\lambda^2+\omega^2\right)\right] - t_C\left(\lambda^2+\omega^2\right)\left(\lambda^2\omega^2 - 2\lambda\rho + \omega^4\right)\right\}$
$A_3 = -4\lambda\rho\left\{m_C\left(\lambda^2+\omega^2\right)^2 + \lambda\left[-\lambda^3\omega^2 - \lambda\omega^4 + 2\rho\omega^2 + \lambda^2\left(\rho + t_C\omega^2\right) + t_C\omega^4\right]\right\}$
$B_3 = -\omega\left(\lambda^2+\omega^2\right)\left\{\rho\omega^4 + \lambda^5\omega^2 - \lambda^4\rho + 2\lambda^3\omega^4 - 2\lambda^2\rho\omega^2 + 2\lambda\rho^2 + \lambda\omega^6 + m_C\left(\lambda^2+\omega^2\right)\left[-\lambda^3 - \lambda\omega^2 + \rho + t_C\left(\lambda^2+\omega^2\right)\right] - t_C\left(\lambda^2+\omega^2\right)\left(\lambda^2\omega^2 - 2\lambda\rho + \omega^4\right)\right\} +$ $A_4 = 4\lambda\rho\omega\left[-\lambda\omega^2 + \rho + t_C\left(\lambda^2+\omega^2\right)\right]\left\{m_C\left(\lambda^2+\omega^2\right)^2 + \lambda\left[-\lambda^3\omega^2 - \lambda\omega^4 + 2\rho\omega^2 + \lambda^2\left(\rho + t_C\omega^2\right) + t_C\omega^4\right]\right\}$
$B_4 = \omega^2\left(\lambda^2+\omega^2\right)\left[-\lambda\omega^2 + \rho + t_C\left(\lambda^2+\omega^2\right)\right]\left\{\left(\lambda\omega^2 - \rho\right)\left(\lambda^2+\omega^2\right)^2 + 2\lambda\rho^2 - t_C\left(\lambda^2+\omega^2\right)\left(\lambda^2\omega^2 - 2\lambda\rho + \omega^4\right) + m_C\left(\lambda^2+\omega^2\right)\left[-\lambda^3 - \lambda\omega^2 + \rho + t_C\left(\lambda^2+\omega^2\right)\right]\right\}$
$A_5 = 8\lambda^4\rho\omega\left\{m_C\left(\lambda^2+\omega^2\right)^2 + \lambda\left[-\lambda^3\omega^2 - \lambda\omega^4 + 2\rho\omega^2 + \lambda^2\left(\rho + t_C\omega^2\right) + t_C\omega^4\right]\right\}$
$B_5 = -2\left(\lambda^2+\omega^2\right)^2\left[2\lambda^5\rho\omega^2 - 2\lambda^4\rho^2 - 2\lambda^4\omega^6 + 5\lambda^3\rho\omega^4 - 5\lambda^2\rho^2\omega^2 - \lambda^2\omega^8 + 2\lambda\rho^3 + 2\lambda\rho\omega^6 - t_C^2\omega^2\left(\lambda^2+\omega^2\right)\left(\lambda^2\omega^2 - 2\lambda\rho + \omega^4\right)\right] -$ $-2\left(\lambda^2+\omega^2\right)^2\left\{-\rho^2\omega^4 - \lambda^6\omega^4 + t_C\left[2\lambda^5\omega^4 - 5\lambda^4\rho\omega^2 + 2\lambda^3\left(\rho^2 + 2\omega^6\right) - 7\lambda^2\rho\omega^4 + 2\lambda\left(2\rho^2\omega^2 + \omega^8\right) - 2\rho\omega^6\right]\right\} -$ $-2\left(\lambda^2+\omega^2\right)^2 m_C\left[\lambda^6\omega^2 - 2\lambda^5\rho + 2\lambda^4\omega^4 - 4\lambda^3\rho\omega^2 + \lambda^2\left(2\rho^2 + \omega^6\right) - 2\lambda\rho\omega^4 + \rho^2\omega^2 + t_C\left(\lambda^2+\omega^2\right)\left(\omega^2\left(t_C - 2\lambda\right) + 2\rho\right)\right]$
$A_6 = -4\lambda\rho\omega\left[-2\lambda^3 - \lambda\omega^2 + \rho + t_C\left(\lambda^2+\omega^2\right)\right]\left\{m_C\left(\lambda^2+\omega^2\right)^2 + \lambda\left[-\lambda^3\omega^2 - \lambda\omega^4 + 2\rho\omega^2 + \lambda^2\left(\rho + t_C\omega^2\right) + t_C\omega^4\right]\right\}$
$B_6 = \omega^2\left(\lambda^2+\omega^2\right)\left(-2\lambda^8\omega^2 + 8\lambda^7\rho - 5\lambda^6\omega^4 + 16\lambda^5\rho\omega^2 - 9\lambda^4\rho^2 - 4\lambda^4\omega^6 + 10\lambda^3\rho\omega^4 - 8\lambda^2\rho^2\omega^2 - \lambda^2\omega^8 + 2\lambda\rho^3 + 2\lambda\rho\omega^6 - \rho^2\omega^4\right) +$ $+\omega^2\left(\lambda^2+\omega^2\right)^2\left[2\lambda^6 m_C + 3\lambda^4 m_C\omega^2 - 3\lambda^3 m_C\rho + \lambda^2 \mathrm{mC}\omega^4 - 2\lambda m_C\rho\omega^2 + m_C\rho^2 + t_C\left(3\lambda^5\omega^2 - 9\lambda^4\rho + 5\lambda^3\omega^4 - 9\lambda^2\rho\omega^2 + 4\lambda\rho^2 + 2\lambda\omega^6 - 2\rho\omega^4\right)\right] -$ $-\omega^2\left(\lambda^2+\omega^2\right)^3\left[t_C^2\left(\lambda^2\omega^2 - 2\lambda\rho + \omega^4\right) + m_C t_C\left(3\lambda^3 + 2\lambda\omega^2 - 2\rho\right)\right] + \omega^2\left(\lambda^2+\omega^2\right)^4 m_C t_C^2$
$A_7 = 4\lambda\rho\left\{m_C^2\left(\lambda^2+\omega^2\right)^2 + \lambda m_C\left[-\lambda^3\omega^2 - \lambda\omega^4 + 3\rho\omega^2 + \lambda^2\left(2\rho + t_C\omega^2\right) + t_C\omega^4\right] + \rho\left(\lambda^2+\omega^2\right)\left[\rho + \omega^2\left(t_C - \lambda\right)\right]\right\}$
$B_7 = \omega\left(\lambda^2+\omega^2\right)\left[m_C^2\left(\lambda^2+\omega^2\right) - m_C\left(\lambda^2\omega^2 - 2\lambda\rho + \omega^4\right) + \rho^2\right]\left[-\lambda^3 - \lambda\omega^2 + \rho + t_C\left(\lambda^2+\omega^2\right)\right]$
$A_8 = -4\lambda\rho\left\{m_C\left(\lambda^2+\omega^2\right)^2 + \lambda\left[-\lambda^3\omega^2 - \lambda\omega^4 + 2\rho\omega^2 + \lambda^2\left(\rho + t_C\omega^2\right) + t_C\omega^4\right]\right\}$
$B_8 = -\omega\left(\lambda^2+\omega^2\right)\left[-\lambda^2\omega^2 + 2\lambda\rho + m_C\left(\lambda^2+\omega^2\right) - \omega^4\right]\left[-\lambda^3 - \lambda\omega^2 + \rho + t_C\left(\lambda^2+\omega^2\right)\right]$

Table A.1: The coefficients A_i and B_i of Theorem 5 and Lemma 9.

References

[1] S. N. Chow, J. K. Hale, Methods of Bifurcation Theory, Springer-Verlag, New York, 1982.

[2] R. D. Euzébio, J. Llibre, Zero-Hopf bifurcation in a Chua's system, Nonlinear Analysis: Real World Applications 37 (2017) 31–40. doi:10.1016/j.nonrwa.2017.02.002.

[3] A. Mees, L. Chua, The Hopf bifurcation theorem and its applications to nonlinear oscillations in circuits and systems, IEEE Transactions on Circuits and Systems 26 (4) (1979) 235–254. doi:10.1109/tcs.1979.1084636.

[4] J. Sotomayor, L. F. Mello, D. de Carvalho Braga, Stability and Hopf bifurcation in an hexagonal governor system, Nonlinear Analysis: Real World Applications 9 (3) (2008) 889–898. doi:10.1016/j.nonrwa.2007.01.007.

[5] T. Chen, L. Huang, P. Yu, W. Huang, Bifurcation of limit cycles at infinity in piecewise polynomial systems, Nonlinear Analysis: Real World Applications 41 (2018) 82–106. doi:10.1016/j.nonrwa.2017.10.003.

[6] F. Geng, X. Li, Singular orbits and dynamics at infinity of a conjugate Lorenz-like system, Mathematical Modelling and Analysis 20 (2) (2015) 148–167. doi:10.3846/13926292.2015.1019944.

[7] W. Keith, R. Rand, Dynamics of a system exhibiting the global bifurcation of a limit cycle at infinity, International Journal of Non-Linear Mechanics 20 (4) (1985) 325–338. doi:10.1016/0020-7462(85)90040-x.

[8] F. Li, Y. Liu, P. Yu, Bifurcation of limit cycles at infinity in a class of switching systems, Nonlinear Dynamics 88 (1) (2016) 403–414. doi:10.1007/s11071-016-3249-4.

[9] Y. Liu, Analysis of global dynamics in an unusual 3D chaotic system, Nonlinear Dynamics 70 (3) (2012) 2203–2212. doi:10.1007/s11071-012-0610-0.

[10] Y. Liu, Dynamics at infinity and the existence of singularly degenerate heteroclinic cycles in the conjugate Lorenz-type system, Nonlinear Analysis: Real World Applications 13 (6) (2012) 2466–2475. doi:10.1016/j.nonrwa.2012.02.011.

[11] Z. Wei, I. Moroz, Z. Wang, J. C. Sprott, T. Kapitaniak, Dynamics at infinity, degenerate Hopf and zero-Hopf bifurcation for Kingni–Jafari system with hidden attractors, International Journal of Bifurcation and Chaos 26 (07) (2016) 1650125. doi:10.1142/s021812741650125x.

[12] Q. Zhang, Y. Liu, A cubic polynomial system with seven limit cycles at infinity, Applied Mathematics and Computation 177 (1) (2006) 319–329. doi:10.1016/j.amc.2005.11.011.

[13] J. N. Glover, Hopf bifurcations at infinity, Nonlinear Analysis, Theory, Methods & Applications 13 (12) (1989) 1393–1398. doi:10.1016/0362-546x(89)90100-4.

[14] V. S. Kozjakin, M. A. Krasnosel'skii, The method of parameter functionalization in the Hopf bifurcation problem, Nonlinear

Analysis, Theory, Methods & Applications 11 (2) (1987) 149–161. doi:10.1016/0362-546x(87)90095-2.

[15] P. Diamond, N. A. Kuznetsov, D. Rachinskii, On the Hopf bifurcation in control systems with a bounded nonlinearity asymptotically homogeneous at infinity, Journal of Differential Equations 175 (1) (2001) 1–26. doi:10.1006/jdeq.2000.3916.

[16] A. Andronov, A. Vitt, S. Khaikin, Theory of oscillations, Pergamon Press, Oxford, 1966.

[17] N. Levinson, A second order differential equation with singular solutions, The Annals of Mathematics 50 (1) (1949) 127–153. doi:10.2307/1969357.

[18] S. Smale, Finding a horseshoe on the beaches of Rio, The Mathematical Intelligencer 20 (1) (1998) 39–44. doi:10.1007/bf03024399.

[19] B. C. Bao, Q. D. Li, N. Wang, Q. Xu, Multistability in Chua's circuit with two stable node-foci, Chaos: An Interdisciplinary Journal of Nonlinear Science 26 (4) (2016) 043111. doi:10.1063/1.4946813.

[20] E. Freire, M. Ordóñez, E. Ponce, Limit cycle bifurcation from a persistent center at infinity in 3D piecewise linear systems with two zones, in: Trends in Mathematics, Springer International Publishing, 2017, pp. 55–58. doi:10.1007/978-3-319-55642-0_10.

[21] D. Simpson, The instantaneous local transition of a stable equilibrium to a chaotic attractor in piecewise-smooth systems of dif-

ferential equations, Physics Letters A 380 (38) (2016) 3067–3072. doi:10.1016/j.physleta.2016.07.033.

[22] N. V. Stankevich, N. V. Kuznetsov, G. A. Leonov, L. O. Chua, Scenario of the birth of hidden attractors in the Chua's circuit, International Journal of Bifurcation and Chaos 27 (12) (2017) 1730038. doi:10.1142/s0218127417300385.

[23] F. Torres, E. Ponce, E. Freire, V. Carmona, The continuous matching of two stable linear systems can be unstable, Discrete and Continuous Dynamical Systems 16 (3) (2006) 689–703. doi:10.3934/dcds.2006.16.689.

[24] V. Carmona, E. Freire, E. Ponce, J. Ros, F. Torres, Limit cycle bifurcation in 3D continuous piecewise linear systems with two zones. Application to Chua's circuit, International Journal Bifurcation and Chaos 15 (10) (2005) 3153–3164. doi:10.1142/s0218127405014027.

[25] E. Freire, E. Ponce, J. Ros, Limit cycle bifurcation from center in symmetric piecewise-linear systems, Int. J. of Bifurcation and Chaos 09 (05) (1999) 895–907. doi:10.1142/s0218127499000638.

[26] E. Freire, E. Ponce, J. Ros, The focus-center-limit cycle bifurcation in symmetric 3D piecewise linear systems, SIAM Journal of Applied Mathematics 65 (6) (2005) 1933–1951. doi:10.1137/040606107.

[27] E. Ponce, A. Amador, J. Ros, A multiple focus-center-cycle bifurcation in 4D discontinuous piecewise linear memristor oscillators, Nonlinear Dynamics 94 (4) (2018) 3011–3028. doi:10.1007/s11071-018-4541-2.

[28] E. Ponce, J. Ros, E. Vela, Unfolding the fold-Hopf bifurcation in piecewise linear continuous differential systems with symmetry, Physica D: Nonlinear Phenomena 250 (2013) 34–46. doi:10.1016/j.physd.2013.01.010.

[29] E. Freire, E. Ponce, J. Ros, A new methodology for limit cycle bifurcation from infinity in n-dimensional symmetric piecewise linear control systems, Chaos'06, 1st IFAC Conference on Analysis and Control of Chaotic Systems Notes 39 (8). doi:10.3182/20060628-3-fr-3903.00039.

[30] S. Rajasekar, M. Lakshmanan, Period-doubling bifurcations, chaos, phase-locking and devils staircase in a Bonhoeffer-van der Pol oscillator, Physica D: Nonlinear Phenomena 32 (1) (1988) 146–152. doi:10.1016/0167-2789(88)90091-7.

[31] M. Sekikawa, N. Inaba, T. Yoshinaga, T. Hikihara, Period-doubling cascades of canards from the extended Bonhoeffer-van der Pol oscillator, Physics Letters A 374 (36) (2010) 3745–3751. doi:10.1016/j.physleta.2010.07.033.

[32] K. Shimizu, Y. Saito, M. Sekikawa, N. Inaba, Complex mixed-mode oscillations in a Bonhoeffer-van der Pol oscillator under weak periodic perturbation, Physica D: Nonlinear Phenomena 241 (18) (2012) 1518–1526. doi:10.1016/j.physd.2012.05.014.

[33] V. Carmona, E. Freire, E. Ponce, F. Torres, On simplifying and classi-

fying piecewise linear systems, IEEE Trans. Circuits Systems I: Fund. Theory Appl. 49 (2002) 609–620. doi:10.1109/TCSI.2002.1001950.

[34] N. A. Gubar, Investigation of a piecewise linear dynamical system with three parameters, Journal of Applied Mathematics and Mechanics 25 (6) (1961) 1519–1535. doi:10.1016/0021-8928(62)90132-6.

[35] G. Kovatch, A method for the computation of self-sustained oscillations in systems with piecewise linear elements, IEEE Transactions on Automatic Control 8 (4) (1963) 358–365. doi:10.1109/tac.1963.1105598.

[36] G. A. Kriegsmann, The rapid bifurcation of the Wien bridge oscillator, IEEE Transactions on Circuits and Systems 34 (9) (1987) 1093–1096. doi:10.1109/tcs.1987.1086245.

[37] Y. Nishiuchi, T. Ueta, H. Kawakami, Stable torus and its bifurcation phenomena in a simple three-dimensional autonomous circuit, Chaos, Solitons and Fractals 27 (4) (2006) 941–951. doi:10.1016/j.chaos.2005.04.092.

[38] E. Ponce, J. Ros, E. Vela, Analysis, Modelling, Optimization, and Numerical Techniques, Vol. 121, Springer Proceedings in Mathematics and Statistics, Colombia, 2015, Ch. A Unified Approach to Piecewise Linear Hopf and Hopf-Pitchfork Bifurcations, pp. 173–184. doi:10.1007/978-3-319-12583-1_12.

[39] C. Grebogi, E. Ott, S. Pelikan, J. A. Yorke, Strange attractors that are not chaotic, Physica D: Nonlinear Phenomena 13 (1-2) (1984) 261–268. doi:10.1016/0167-2789(84)90282-3.

[40] I. Wolfram Research, Mathematica, Version 11.1, Wolfram Research, Inc., Champaign, Illinois, 2018.